

Pre-clinical investigations of multi-path propagation in transcranial Doppler ultrasound flow phantom

Alexander J. Weir¹, Cheng-Xiang Wang² and Stuart Parks³

Abstract—There are various practical situations in medical applications when pre-clinical investigations must be performed using a simulation environment or test bench prior to human studies. One example is the analysis of propagation channels in Transcranial Doppler (TCD) ultrasound (US), a signal processing challenge requiring the analysis of data from US waves scattered in three dimensions (3D). When examining the effects of scatterers in such channels, it is common to use a data acquisition test bench and a Doppler flow phantom. Such medical phantoms are frequently required to verify image and signal processing systems, and are often used to support algorithm development for a wide range of imaging and blood flow assessments. In this paper we describe a TCD simulation environment for the acquisition, investigation and pre-clinical data analysis of multi-path propagation in TCD US systems. This is demonstrated by comparing the anticipated theoretical and simulation channel statistics with the measured acoustic characteristics in terms of the probability distribution and autocorrelation functions.

I. INTRODUCTION

Transcranial Doppler (TCD) ultrasound (US) [1] [2] is a low frequency (2 MHz) pulsed Doppler US system used to interrogate the intra-cranial arterial anatomy for specialized clinical applications such as detection of intra-cranial stenosis, analysis of secondary blood flow channels, intra-operative monitoring and measurement of dynamic cerebrovascular response. The focus of the system discussed in this paper is to improve understanding of the propagation channel effects in order to enhance detection of micro embolic signals (MES) for the diagnosis and prediction of embolic complications in stroke-risk patients. In order to improve our ability to assess the risk of patients vulnerable to ischemic stroke, there is general acceptance that clinical examination using TCD US should move from simply quantifying embolization rates to a qualitative analysis of embolization events using optimized signal processing techniques and more extensive time windows [3].

In recent years there has been much interest in the use of chirp signals, coded excitation and pseudo noise (PN) codes [4]–[7] which use coded pulse sequences and digital signal processing (DSP) techniques to improve the sensitivity and

reliability of detection, and subsequently the ability to track blood flow and emboli motion in TCD systems. However, lessons from radio communications [8] have shown that successful design of such techniques rely upon a thorough knowledge of the channel and the multi-path propagation effects resulting from the reflection, diffraction and scattering on the received signal by the medium (fig.1). As a pre-clinical first step in analyzing the TCD propagation channel, there is a requirement for the development and characterization of a simulation environment based on an US flow phantom, with physiological tissue and blood equivalence. This simulation environment will provide a data acquisition system for investigation and analysis of the TCD channel, in terms of the mean, variance, probability distribution function (PDF) and autocorrelation function (ACF).

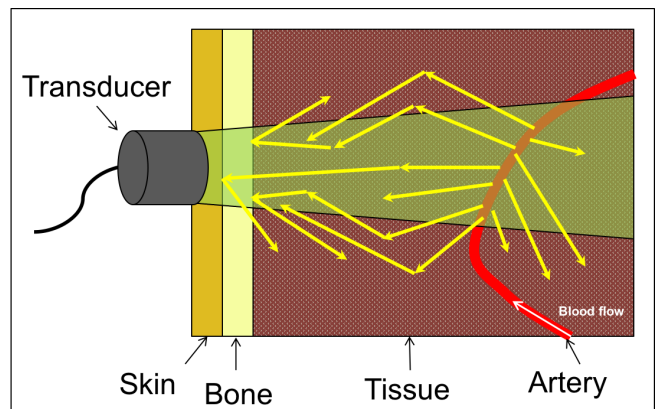


Fig. 1: A schematic showing the effects of scattering, diffraction and reflection on transcranial Doppler ultrasound propagation channel.

This paper is organized as follows: Section II describes the materials, design and methods used for data acquisition from the channel. Section III analyzes the acoustic characteristics in terms of the theoretical and measured probability distribution functions (PDFs) and autocorrelation functions (ACFs). Section IV examines the performance of the flow phantom test bench and the level of agreement with the theoretical characteristics. The paper concludes in section V.

II. MATERIALS AND METHODS

A. Transcranial Doppler Simulation Test Bench

A test bench was created to analyse and compare the theoretical and measured acoustic characteristics of a TCD

¹A.J. Weir is with the Medical Devices Unit, Department of Clinical Physics, West Glasgow Ambulatory Care Hospital, Glasgow, United Kingdom and the School of Engineering and Physical Science, Heriot-Watt University, Edinburgh, United Kingdom. alexander.weir@nhs.net

²C.-X. Wang is with School of Engineering and Physical Science, Heriot-Watt University, Edinburgh, United Kingdom. cheng-xiang.wang@hw.ac.uk

³S. Parks is with the Medical Devices Unit, Department of Clinical Physics, West Glasgow Ambulatory Care Hospital, Glasgow, United Kingdom. stuart.parks@nhs.net

US propagation channel (fig. 2). The test bench consists of

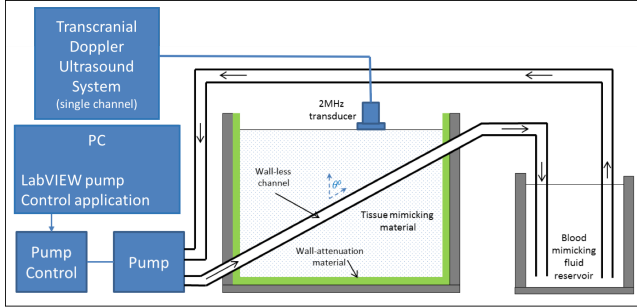


Fig. 2: A schematic of the TCD ultrasound simulation test bench.

a portable, 2 MHz, power-motion or single-channel TCD (PMD 100, *Spencer Technologies*) US system [9], a windows computer running LabVIEWTM (*National Instruments*), a pump and pump-controller (*Department of Clinical Physics & Bioengineering, NHS Greater Glasgow and Clyde*) capable of operating with constant and pulsatile flow, connected to a 68-pin data acquisition (DAQ) PC card via a shielded connector block (*National Instruments SCB-68*), a poly vinyl alcohol (PVA) cryogel flow phantom [10] and reservoir of blood mimicking fluid [11]. An image of the test bench is shown in fig. 3.

The LabVIEWTM application was used to synthesize a blood flow waveform and drive the pump using pulsatile and constant flow using the DAQ and pump controller. This process circulated blood mimicking fluid through the flow phantom whilst a single-element 2 MHz transducer was placed on the flow phantom to capture Doppler US signals.

When used in pulsatile mode, the blood flow waveform

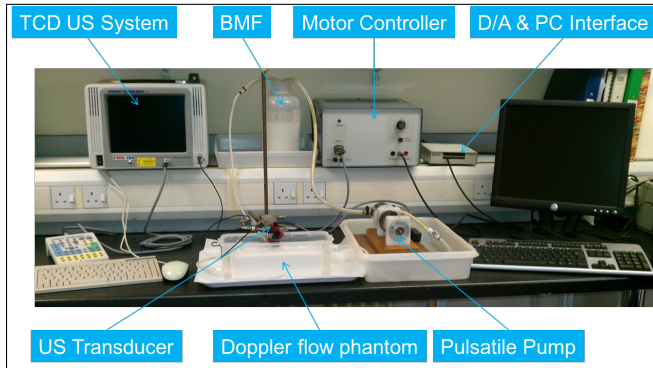


Fig. 3: A picture of the TCD ultrasound simulation test bench used in the experiment.

was derived from the average statistical properties of TCD signal recordings in a database of over seventy anonymized and depersonalized patient examinations.

B. Data Acquisition

If we consider the schematic shown in fig.1, the US waves are transmitted by the transducer and those echoes received from stationary tissue can be considered to exhibit

the same frequency and phase as the transmitted signal. However, echoes received from scatterers (i.e. moving tissue and fluids) will exhibit slight differences in time and/or phase. From these differences the Doppler frequency is obtained which can then be processed to produce a Doppler sonogram. For the case of Doppler shift in US, the Doppler frequency f_D can be expressed by

$$f_D = 2 \left(\frac{V_0}{\lambda_c} \right) \cos(\theta) = 2 \left(\frac{V_0}{c} \right) \cos(\theta) f_c \quad (1)$$

where V_0 is the velocity of the back scattering blood, λ_c is the US insonation wavelength, c is the speed of sound in the medium, f_c is the US insonation frequency and θ is the angle of incidence.

The optimal f_c for studying the intra-cranial arteries using TCD US systems is ≤ 2 MHz [2] [12]. This is essentially a compromise between signal-to-noise ratio and desired penetration depth. At 2 MHz a TCD system can penetrate the trans-temporal acoustic window, a region of the skull where the bone thins to around 2-3 mm. The maximum Doppler frequency shift detectable at the transducer occurs when the angle of incidence is zero, as expressed by

$$f_{D_{max}} = 2 \left(\frac{V_0}{\lambda_c} \right) = 2 \left(\frac{V_0}{c} \right) f_c \quad (2)$$

and from (1) the observed f_D is given by

$$f_D = f_{D_{max}} \cos(\theta). \quad (3)$$

In this study θ is 60° . If we approximate c to 1500 ms^{-1} then λ_c can be approximated to 0.75 mm . If we then estimate the peak systolic pulsatile blood flow velocity to be in the region of 0.8 ms^{-1} in the middle cerebral artery, then $f_{D_{max}}$ can be approximated to 2 KHz using equation (2). The Doppler shift lies, therefore, within the human audible range.

Using the TCD US system in single channel mode whilst insonating at a depth of approximately 40 mm and using 10% of maximum power, raw Doppler signals were acquired from the flow phantom and exported as audio files consisting of 32 bit floating point data sampled at a frequency of 44100 Hz. An example of the power m-mode and spectrogram display when the flow phantom pump was operated at a constant flow rate is shown in fig.4.

III. ACOUSTIC CHARACTERISTICS

Sample datasets were captured from the blood flow phantom whilst operating with both constant and pulsatile blood flow profiles. MatlabTM (MathWorks Inc.) scripts were developed to analyze the received signals and determine some initial statistical properties of the flow phantom in terms of the PDF and ACF. These statistical properties were compared with a Rayleigh based fading model consisting of a 3D half-spheroid theoretical reference and simulation model [13].

Blood is a highly complex fluid that is composed of objects of differing shapes and sizes, such as plasma, leukocytes, erythrocytes and platelets. The overwhelmingly dominant ultrasonic scatterers are the erythrocytes or red blood cells

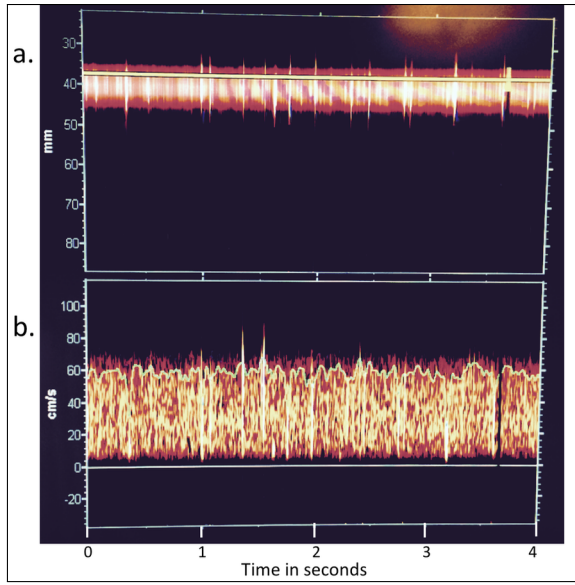


Fig. 4: The TCD blood flow displays captured using a single-channel PMD 100 TCD US system whilst the flow phantom pump was operating with a constant flow rate of 0.6 m s^{-1} . (a) The power m-mode display shows the insonation gate depth in mm on the vertical axis in a 4-second time window on the horizontal axis. The power of the Doppler shift signal at specific depths is a function of image intensity [9]. (b) The concurrent flow spectrogram at the insonation gate depth with the flow rate in cm/s on the vertical axis and a 4-second time window on the horizontal axis.

(RBC); biconcave, discoidal cells of approximately $8 \mu\text{m}$ in diameter and $2 \mu\text{m}$ thick. An individual RBC is two orders of magnitude smaller than the US wavelength and the backscatter of blood from ultrasound reflection increases as the fourth power of frequency; thus exhibiting Rayleigh scattering [14] and justifying the choice of a Rayleigh fading model for statistical comparison.

A. Probability Distribution Function

The normalized PDF of the received flow phantom signal is shown in fig.5. For comparison, it has been plotted with the PDF of Gaussian white noise and the normal distribution $P_\mu(x)$, where

$$p_\mu(x) = \frac{1}{\sqrt{2\pi}\sigma_\mu} \exp\left[-\frac{(x - m_\mu)^2}{2\sigma_\mu^2}\right]. \quad (4)$$

In equation (4), the mean (m_μ) is zero and the standard deviation (σ) is one. It is evident from the close agreement of the waveforms that the flow phantom signal tends, under normal conditions, to be Gaussian and the process can be treated as a Gaussian random process.

B. Autocorrelation Function

As reported in [13] and in accordance with predictions from the Rayleigh fading model, the TCD fading channel should provide an autocorrelation function in the form of a zeroth-order Bessel function of the first kind ($J_0(\cdot)$). The

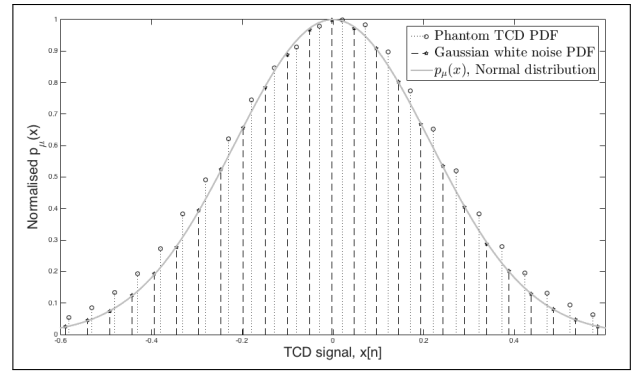


Fig. 5: The normalized probability density function of the sampled and averaged transcranial Doppler ultrasound signal recording.

ACF can be expressed as the integral of the product of the baseband signal and the joint density function [15], given by

$$\phi_{rr}(\tau) = \frac{\Omega_p}{2} \int_0^{\pi/2} J_0(2\pi f_m \tau \cos \beta) \cos \beta d\beta \quad (5)$$

where Ω_p is the total received power, f_m is the maximum Doppler frequency, β is the elevation angle of arrival (EAOA). A simulation model can be derived which emulates signals received at the transducer [13].

The normalized ACFs of the theoretical and simulated case are plotted for comparison with the ACFs of the received signals in fig.6. Two classes of received signal were observed. Firstly, the case when the flow phantom pump was operated at a constant flow rate and a mean blood flow velocity of approximately 0.6 m s^{-1} . Secondly, when the flow phantom pump was operated with a pulsatile flow profile and a peak blood flow velocity of 0.8 m s^{-1} .

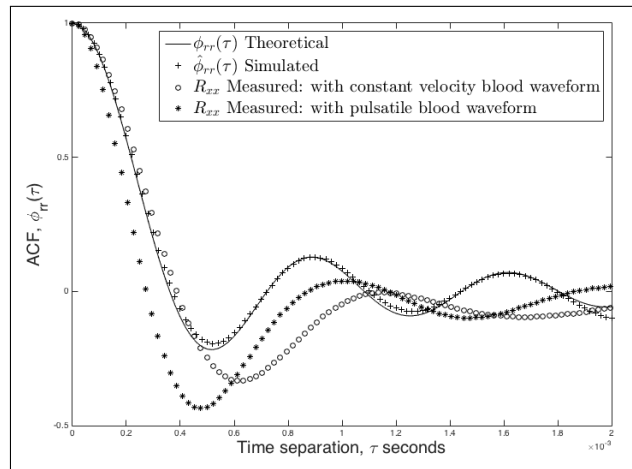


Fig. 6: The theoretical, simulated and measured ACF, with a constant flow rate and a mean blood flow velocity of approximately 0.6 m s^{-1} , and a pulsatile flow profile and a peak blood flow velocity of approximately 0.8 m s^{-1} .

IV. RESULTS

The normalized probability distribution derived from the measured results shows reasonably close agreement with the normal distribution and Gaussian white noise process. In this respect, the measured results were anticipated and the TCD US propagation channel can be treated as a Gaussian random process. Indeed, the slight disagreement can, most likely, be attributed to the recording sample lengths and it can reasonably be expected that analysis of much longer contiguous datasets would produce ever closer agreement.

The normalized autocorrelation function derived from the measured results do not show satisfactory agreement with the theoretical and simulated 3D half-spheroid models. In the case when a pulsatile flow profile was used this was at least expected. The theoretical and simulated model parameters assume that blood flow motion is a constant velocity. Blood flow velocities for a normal adult range from 100 cm.s^{-1} to 1 cm.s^{-1} , and the pulsatile flow profile used in the experiment was based on analysis of measured data from the middle cerebral artery (MCA) and varies between a systolic peak of 80 cm.s^{-1} and a diastolic peak of 20 cm.s^{-1} .

In the case when a constant flow velocity was used, disagreement with the theoretical and simulated models was not anticipated. A comparison of the waveforms shows the ACF derived from the measured signal begins with close agreement to the theoretical and simulated results until approximately 0.5 msec, then diverges with a lower amplitude and frequency. The initial agreement confirms that the fundamental frequencies of the theoretical, simulated and measured results are equal, however the divergence shows the frequency and amplitude of harmonics do not match the models.

There are a number of possible reasons for this; the 3D geometry of the half-spheroid model may not be suitably accurate, the effects of reflection and refraction from the base and side walls of the phantom may be a source of interference, or the flow system and pump may produce artefact's in the measured signal. There is some evidence of the latter in the m-mode and blood flow displays shown in fig.4. Close examination of the waveform suggests that the flow system may certainly be one possible source of error. The ripple on the flow velocity (approximately $\pm 10 \text{ m.s}^{-1}$) and evidence of short peaks of interference suggest that, despite careful adherence to [11], the fluid may not have a sufficiently constant or laminar flow profile, and some turbulence may be the cause of some inaccuracy.

V. CONCLUSIONS

In this paper, we have investigated a TCD test bench for the acquisition, investigation and pre-clinical data analysis of multi-path propagation in TCD US systems. The test bench has been used successfully to obtain data for analysis of the initial statistical properties of the TCD signal. Although the PDF obtained confirms the TCD signal can be treated as a Gaussian random process, the ACF obtained did not fully agree with previously derived theoretical and simulation models. There is evidence in the results that suggest a

comparison of this sort is highly sensitive to any non-laminar flow in the phantom and further investigations are required, both with the model derivations, and the test environment in order to achieve a more satisfactory comparison of the ACF, and to have more confidence in the validity of the theoretical and simulation models.

In the case of the theoretical and simulation models specifically, although it may be reasonable to consider the theoretical biological properties of tissue and blood well matched to a Rayleigh fading process, the interaction of ultrasound with blood is complex. A useful extension to the approach described would be to consider a more flexible Ricean fading model for investigating, analysing and comparing the effect of a significant line-of-sight component in the received signal. Further, the variable motion of pulsatile blood flow should also be considered. Finally, in order to support clinical analysis, a model may be required which supports both time-varying and motion-varying cases in order to describe the channel correlation properties accurately.

REFERENCES

- [1] R. Aaslid, T.-M. Markwalder, and H. Nornes, "Noninvasive transcranial doppler ultrasound recording of flow velocity in basal cerebral arteries," *Journal of neurosurgery*, vol. 57, no. 6, pp. 769–774, 1982.
- [2] H. S. Markus, "Transcranial doppler ultrasound," *Journal of Neurology, Neurosurgery & Psychiatry*, vol. 67, no. 2, pp. 135–137, 1999.
- [3] T. Idicula and L. Thomassen, *Microemboli Monitoring in Ischemic Stroke*. INTECH Open Access Publisher, 2012.
- [4] J. Cowe, J. Gittins, and D. H. Evans, "Improving performance of pulse compression in a doppler ultrasound system using amplitude modulated chirps and wiener filtering," *Ultrasound in medicine & biology*, vol. 34, no. 2, pp. 326–333, 2008.
- [5] J. Cowe, E. Boni, S. Ricci, P. Tortoli, and D. Evans, "Coded excitation can provide simultaneous improvements in sensitivity and axial resolution in doppler ultrasound systems," in *Ultrasonics Symposium (IUS), 2010 IEEE*, pp. 2286–2290, IEEE, 2010.
- [6] X. Lei, Z. Heng, and G. Shangkai, "Barker code in ted ultrasound systems to improve the sensitivity of emboli detection," *Ultrasound in medicine & biology*, vol. 35, no. 1, pp. 94–101, 2009.
- [7] J. Li, X. Diao, K. Zhan, and Z. Qin, "A full digital design of ted ultrasound system using normal pulse and coded excitation," in *1st Global Conference on Biomedical Engineering & 9th Asian-Pacific Conference on Medical and Biological Engineering*, pp. 136–139, Springer, 2015.
- [8] M. Patzold, *Mobile fading channels*. John Wiley & Sons, Inc., 2003.
- [9] M. A. Moehring and M. P. Spencer, "Power m-mode doppler (pmd) for observing cerebral blood flow and tracking emboli," *Ultrasound in medicine & biology*, vol. 28, no. 1, pp. 49–57, 2002.
- [10] A. J. Weir, R. Sayer, C.-X. Wang, and S. Parks, "A wall-less poly (vinyl alcohol) cryogel flow phantom with accurate scattering properties for transcranial doppler ultrasound propagation channels analysis," in *Engineering in Medicine and Biology Society (EMBC), 2015 37th Annual International Conference of the IEEE*, pp. 2709–2712, IEEE, 2015.
- [11] I. E. Commission *et al.*, *Ultrasonics: Flow Measurement Systems; Flow Test Object; International Standard*. IEC, 2001.
- [12] R. Aaslid, *Transcranial doppler sonography*. Springer Science & Business Media, 2012.
- [13] A. Weir, C.-X. Wang, and S. Parks, "3-d half-spheroid models for transcranial doppler ultrasound propagation channels," in *Biomedical and Health Informatics (BHI), 2014 IEEE-EMBS International Conference on*, pp. 728–731, IEEE, 2014.
- [14] M. A. Moehring, "Fundamental concepts regarding sizing and discrimination of air bubbles and red cell aggregates using pulsed-doppler ultrasound," *Echocardiography*, vol. 13, no. 5, pp. 567–572, 1996.
- [15] Q. Yao and M. Patzold, "Spatial-temporal characteristics of a half-spheroid model and its corresponding simulation model," in *Vehicular Technology Conference, 2004. VTC 2004-Spring. 2004 IEEE 59th*, vol. 1, pp. 147–151, IEEE, 2004.